Fracture and buckling of piezoelectric nanowires subject to an electric field

Jin Zhang, Chengyuan Wang, and Sondipon Adhikari

Citation: J. Appl. Phys. **114**, 174306 (2013); doi: 10.1063/1.4829277
View online: http://dx.doi.org/10.1063/1.4829277
View Table of Contents: http://jap.aip.org/resource/1/JAPIAU/v114/i17
Published by the AIP Publishing LLC.

JOURNAL OF APPLIED PHYSICS **114**, 174306 (2013)

Fracture and buckling of piezoelectric nanowires subject to an electric field

Jin Zhang, Chengyuan Wang,[a] and Sondipon Adhikari
College of Engineering, Swansea University, Singleton Park, Swansea, Wales SA2 8PP, United Kingdom

(Received 7 August 2013; accepted 22 October 2013; published online 6 November 2013)

Fracture and buckling are major failure modes of thin and long nanowires (NWs), which could be affected significantly by an electric field when piezoelectricity is involved in the NWs. This paper aims to examine the issue based on the molecular dynamics simulations, where the gallium nitride (GaN) NWs are taken as an example. The results show that the influence of the electric field is strong for the fracture and the critical buckling strains, detectable for the fracture strength but almost negligible for the critical buckling stress. In addition, the reversed effects are achieved for the fracture and the critical buckling strains. Subsequently, the Timoshenko beam model is utilized to account for the effect of the electric field on the axial buckling of the GaN NWs, where nonlocal effect is observed and characterized by the nonlocal coefficient $e_0a = 1.1$ nm. The results show that the fracture and buckling of piezoelectric NWs can be controlled by applying an electric field. © *2013 AIP Publishing LLC*. [http://dx.doi.org/10.1063/1.4829277]

I. INTRODUCTION

In the past decade, one-dimensional (1D) nanomaterials have offered an excellent platform for basic scientific research in a nanoscale world and potential applications in the nanoelectromechanical systems (NEMS). Among these nanomaterials, the wurtzite family materials, especially the zinc oxide (ZnO) and gallium nitride (GaN), have received considerable attention primarily due to the synergy of their piezoelectric and semiconducting properties. The 1D ZnO and GaN nanostructures, e.g., nanowires (NWs) and nanobelts (NBs), have been used as building blocks of innovative nanodevices, such as nanosensors (actuators),[1,2] nanoresonators,[3] and nanodiodes.[4] In these applications, NWs are usually subjected to tension or compression when being in operation or due to thermal or lattice mismatch between NWs and the materials in environment. It is well known that for thin and long NWs compression may induce the buckling while tension may cause the fracture of the nanostructures. As a result, fracture and buckling are major failure modes of the NWs, which would substantially affect the performance of NW-based nanodevices and nanoelectronics. It is thus of great interest to study the fracture and bulking of the NWs.

Up till now, the buckling and fracture have been studied extensively for piezoelectric GaN and ZnO NWs and NBs,[5–9] where the experimental techniques[5,6,9] and simulation methods, e.g., molecular dynamics simulations (MDS)[7,8] were employed. We noted that the existing studies were mainly focused on the fundamental behaviour of the buckling and fracture but little has been done to investigate the coupling effect of piezoelectric and mechanical properties. On the other hand, our recent study[10] revealed that the stresses and critical buckling strain of carbon nanotube-ZnO composite NWs depends sensitively on the applied electric voltage due to the piezoelectric effect of ZnO. The results suggest that an electric field may significantly affect the fracture and buckling behaviour of piezoelectric NWs.

Inspired by this idea, we are interested in quantifying the influence exerted by an electric field on the fracture and buckling of piezoelectric NWs and capturing the physics behind the obtained electric field effect. To this end, we have performed the MDS, where the fracture and critical buckling stresses and strains are measured for the GaN NWs as a function of the electric field strength. In addition, effort is invested to account for the physics of the observed phenomena by using the continuum mechanics models. The results suggest that piezoelectricity can be employed to maintain the structural integrity and stability of the 1D building blocks in a nanoworld.

II. SIMULATION METHOD

In this paper we consider the most common GaN NW whose growth direction is along the [0001] crystalline direction. Initially, Ga and N atoms are arrayed in a single crystalline wurtzite structure with the lattice constants $a = 3.19$ Å and $c = 5.20$ Å.[11] The NWs have hexagonal cross sections with a six-fold symmetry and $\{01\bar{1}0\}$ lateral surfaces. Such shapes have been observed in GaN NWs grown by metalorganic chemical vapor deposition.[8] The NWs studied here have a length $L_0 = 25$ nm, which is sufficient to avoid image effects, and radius $R = 1.5$ nm as shown in Fig. 1.

The classical MDS was employed in this work and the NVT ensemble (constant Number of particles, Volume and Temperature) was employed to update the positions and velocities of the atoms after each time step by using the Nosé-Hoover temperature thermostat.[12] The interactions between Ga-Ga, N-N, and Ga-N were described by the Stillinger-Weber (SW) potential,[13] which is obtained based on a two-body term φ_2 and a three-body term φ_3:

$$\varphi_2(r_{ij}) = A\delta\left(B\left(\frac{r_{ij}}{d}\right)^{-4} - 1\right)\exp\left(\left(\frac{r_{ij}}{d} - \alpha\right)^{-1}\right), \quad \frac{r_{ij}}{d} < \alpha, \tag{1a}$$

[a]Author to whom correspondence should be addressed. Electronic mail: chengyuan.wang@swansea.ac.uk.

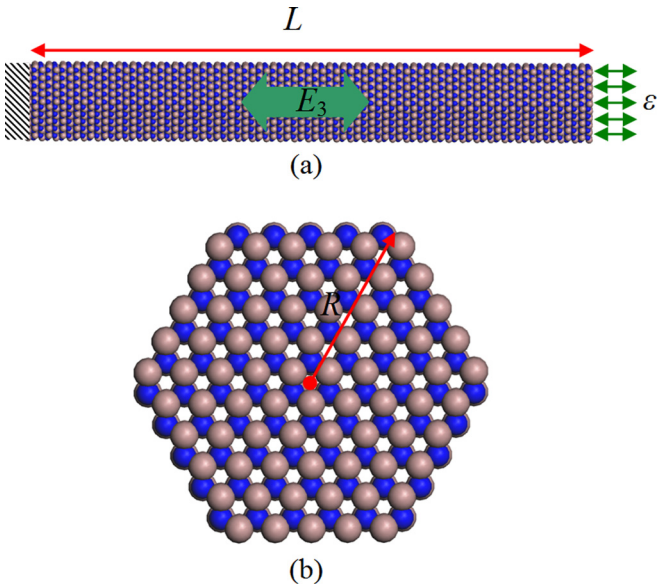

FIG. 1. (a) Molecular representation of the GaN NW studied here, which is subject to an electric field E_3 and strain ε applied in the axial direction of the GaN NW. (b) Cross-section of the GaN NW.

$$\varphi_2(r_{ij}) = 0, \quad \frac{r_{ij}}{d} \geq \alpha, \tag{1b}$$

$$\varphi_3(r_{ij}, r_{ik}, \theta_{ijk}) = \delta\lambda \exp(\gamma(r_{ij} - \alpha)^{-1} + \gamma(r_{ik} - \alpha)^{-1})\left(\cos\theta_{ijk} + \frac{1}{3}\right)^2. \tag{1c}$$

Here, subscripts i, j, and k represent the different atoms in the system. δ is the cohesive energy of the bond. d is the length unit. α represents the cutoff distance. r_{ij} is the length of the bond ij. θ_{ijk} is the angle formed by the ji and the jk bonds. Other parameters, A, B, and γ are dimensionless fitting parameters adjusted to match the material properties. The values used in this study were taken from Ref. 11. The SW potentials have been used to reproduce bulk structures and mechanical properties; they have been successfully employed to evaluate the elastic properties, piezoelectric properties, fracture, and buckling of single-crystal GaN NWs.[7,8,14,15] These calculations have demonstrated that the empirical SW potentials for GaN can be employed to study the mechanical properties of single-crystal GaN structures. In addition, the potentials can handle dangling bonds, wrong bonds, and excess bonds in bulk GaN very well. Therefore, these potentials are proven to be reliable in characterizing the mechanical responses of GaN NWs.

The simulation process is done in the following procedure: first relaxed the initial configuration to reach the equilibrium state (100 ps was used in this work); after the initial relaxation we fixed the two ends of the NWs; then applied the external displacements or/and an electric field along the axial direction (measured by E_3) as shown in Fig. 1(a), and this electric field can produce an external force $f_i = q_i E_3$ on ion i with q_i being the charge on ion i (+3e for Ga^{3+} and −3e for N^{3-}); finally relaxed the NW to reach a new equilibrium state and accordingly, a new configuration. Here all MDS were conducted using the large-scale atomic/molecular massively parallel simulator (LAMMPS)[16] under the room temperature ($T = 300$ K) and without periodic boundary conditions. The axial stress σ on the GaN NW was taken as the arithmetic mean of the local stresses on all atoms, as follows:

$$\sigma = \frac{1}{N}\sum_{i=1}^{N}\frac{1}{V_i}\left(m_i v_z^i v_z^i + \frac{1}{2}\sum_{j\neq i}^{N} F_z^{ij} r_z^{ij}\right), \tag{2}$$

where m_i is the mass of atom i, v_z^i is the velocity component in the axial direction of atom i, F_z^{ij} refers to the axial component of the interatomic force between atoms i and j, r_z^{ij} is the interatomic distance in the axial direction between atoms i and j, V_i refers to the volume of atom i, which is assumed as a hard sphere in a closely packed undeformed crystal structure, and N is the number of atoms.

III. FRACTURE OF PIEZOELECTRIC NWs

In this section, let us first study the fracture of piezoelectric NWs subjected to an electric field. The emphasis will be placed on the effect of piezoelectricity on the fracture behaviour, i.e., how an electric field affects the fracture behaviour of piezoelectric NWs. To reach this goal, the axial stress-strain relation for GaN NWs is plotted in Fig. 2 where the electric field strength varies from -0.4×10^5 kV/cm to 0.4×10^5kV/cm. In Fig. 2, the axial strain ε for the NWs are calculated by $\varepsilon = (L - L_0)/L_0$, where L and L_0 are the lengths of an NW after and before the deformation, respectively. The images of the NW at different stages are shown in Fig. 3, which correspond to points A, B, and C on the stress-strain curve in Fig. 2.

It can be seen from Fig. 2 that at low strain ($\varepsilon \leq 0.05$), the stress-strain relationship follows Hooke's law, i.e., the stress increases linearly with increasing strain. Here, it is also noted that when an electric field is applied the stress-strain curve starts from (σ_0, 0), where the initial strain is zero while the initial stress σ_0 is nonzero as the NW is pre-stressed by an electric field due to the piezoelectric effect. Beyond this linear region ($\varepsilon > 0.05$) the stress continues to

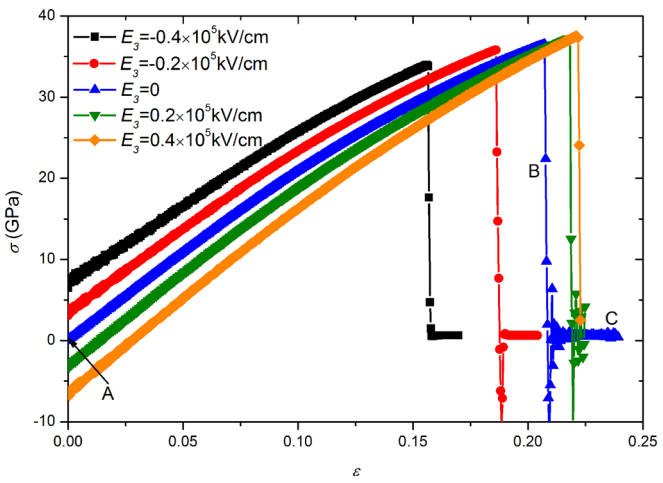

FIG. 2. Stress-strain curves for GaN NWs under a tension and different electric field strengths.

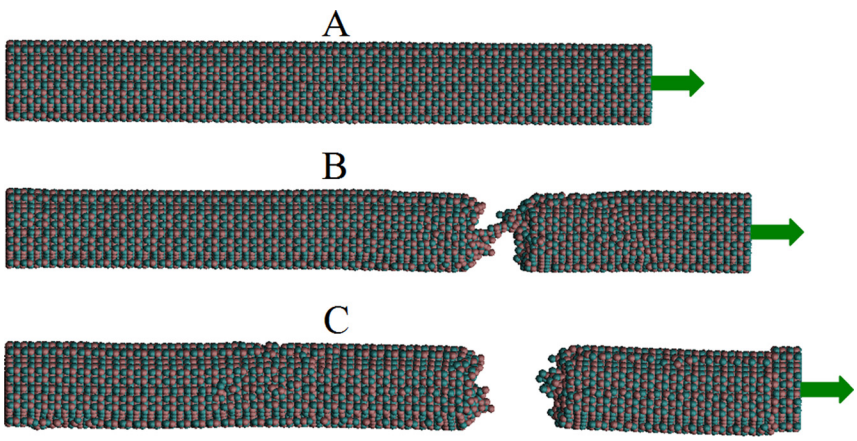

FIG. 3. Structures of GaN NWs under a tension from points A to C in Fig. 2.

increase with growing strain until the stress and strain approach their threshold values, i.e., fracture strength and fracture strain, respectively. After this critical point, a sudden jump of the stress (to zero) is observed with almost no further increase in strain. This indicates the brittle fracture of the GaN NWs, which is also observed in an experiment,[9] and the brittle fracture was also observed in another important semiconductor and piezoelectric NWs, ZnO NWs.[17,18] From Fig. 2, the applied electric field is found to have no influence on the fracture mode of GaN NWs. However, many other factors, e.g., temperature, strain rate and sample dimension may affect the fracture mode of NWs. At the low temperature the semiconductor NWs, e.g., silicon (Si), ZnO, and GaN NWs fail through brittle fracture, but under a high temperature they tend to be ductile.[8,19,20] The fracture mode of semiconductor NWs also depends on the strain rate, e.g., Zheng *et al.*[21] showed the ductile plastic dislocation in Si NWs and pointed out that brittle characters of Si NWs should happen in a fast strain rate. This point was also made by Wang *et al.*[8] in their MDS of GaN NWs. According to their results, the failure of GaN NWs can transfer from the brittle fracture to the ductile fracture as the strain rate decreases. Recently, the size-dependence of fracture mode has been observed not only in the metallic NWs but also in the semiconductor NWs. For example, the fracture of the metallic NWs (e.g., copper and gold NWs) were found to transfer from ductile type to brittle type when their length-to-diameter ratio is larger than ~100.[22] According to the MDS by Kang and Cai, the [110] Si NWs with diameters smaller than 4 nm were found to fail by a ductile fracture at the room temperature, while those with diameters larger than 4 nm then experience a brittle fracture.[19] In addition, through tensile experiments, Han *et al.* reported brittle to ductile transition occurs around 60 nm diameter for [110] Si NWs.[23] Consistent with previous studies of Si NWs, a most recent MDS study[20] showed that under a high temperature the failure of the ZnO NWs transfers from the brittle fracture to the ductile fracture as their diameters decrease.

The evolutions of the molecular structures of GaN NWs in the tensile test are shown in Fig. 3 when there is no electric field. Below the fracture strain, the atomic bonds of the NWs are stretched but still preserve their fourfold coordination. At this stage, no structural defects are found in the NW. With further elongation, the bond breakage occurs in the outmost layer and then propagates rapidly towards the centre as the strain increases. The shearing and necking phenomenon, however, has not been observed for GaN NWs in the MDS. This is in accordance with the aforementioned brittle rapture shown in Fig. 2. Further, the fracture strength and the fracture strain of the GaN NW under tension are plotted in Fig. 4 as a function of the applied electric field. It can be seen from Fig. 4 that the fracture strain increases by around 42% as the applied electric field increases from -0.4×10^5kV/cm to 0.4×10^5kV/cm, meanwhile the fracture strength increases only by about 10%. This observation shows that an electric field has strong influence on the fracture strain. In particular, a negative electric field will decrease the fracture strain, while a positive one will increase it. The effect of electric field on the fracture strain can be possibly explained by the initial stress σ_0 generated by the electric field via the piezoelectric effect. The fracture strength and the absorption energy of a crystal are mainly determined by its molecular structure and atom-atom potential. Therefore, their magnitudes remain nearly constant independent of the electric field. However, in the process of elongation extra work has to be done to resist the negative initial stress due to the electric field. This leads to the increased energy absorption that is proportional to the product of fracture strength and strain. Naturally, the increased energy absorption gives larger fracture strains if the fracture strength is nearly constant. The reverse effect of the positive initial stress can be understood based on the same theory.

From above results, the elastic and piezoelectric properties can also be obtained for the GaN NWs. For example, the axial stress is plotted as a function of strain (at $\varepsilon \leq 0.02$ and $E_3 = 0$) in Fig. 5(a), where the Young's modulus E is represented by the slope of the curve $\sigma - \varepsilon$ and is calculated as 209 GPa. The value is found to be 30% lower than 311 GPa of bulk GaN due to the effect of the surface elasticity.[24] The piezoelectric constant e_{33} is also of major concerns for quasi 1D piezoelectric NWs and is defined by $e_{33} = -\partial\sigma/\partial E_3$.[25] Thus, e_{33} of GaN NWS is represented by the negative slope of the $\sigma - E_3$ curve in Fig. 5(b). The value measured for GaN NWs is 1.8 C/m^2, which is more than two times as much as 0.73 C/m^2 achieved for bulk GaN. The effect of the surface piezoelectricity should be responsible for the discrepancy.[15,26] These fundamental material properties in the constitutive relations of the materials will be utilized latter in

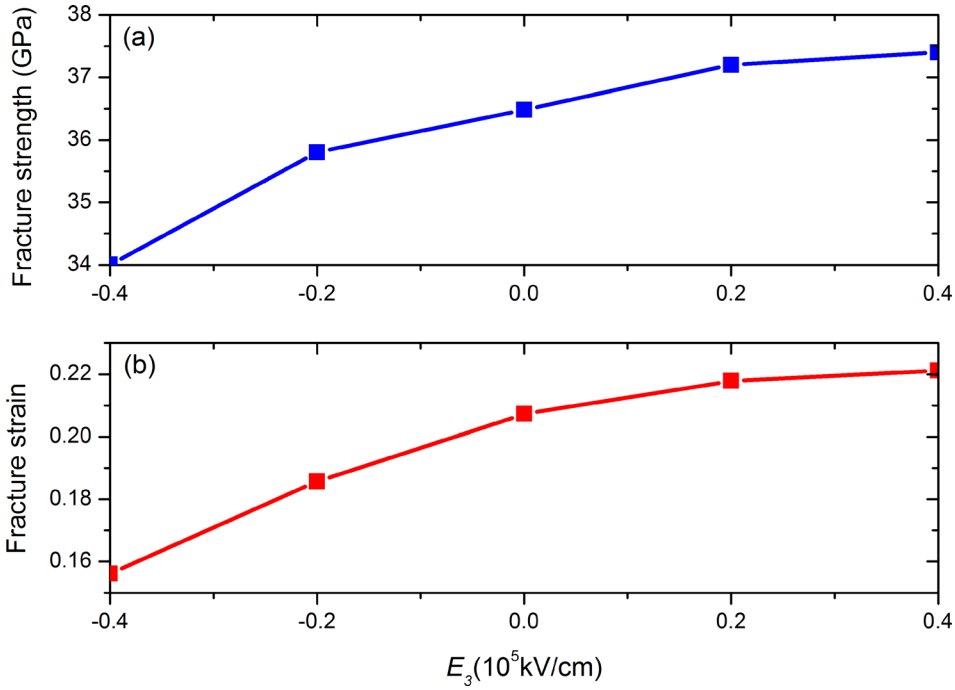

FIG. 4. (a) The fracture strength and (b) the fracture strain as a function of the electric field strength E_3.

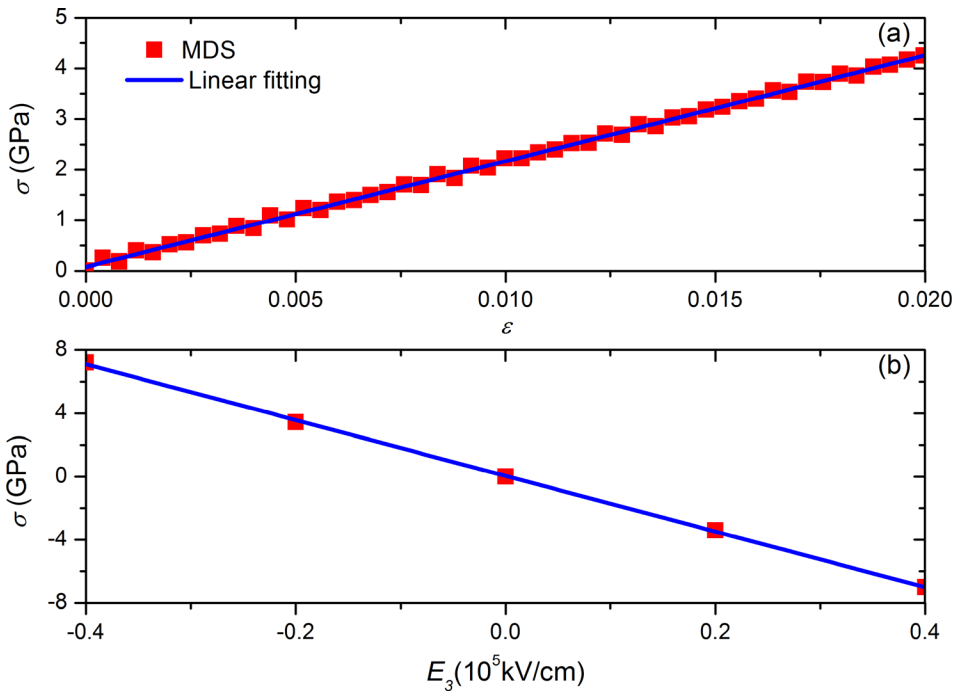

FIG. 5. (a) The stress-strain curve and (b) the stress-electric field strength curve for the GaN NW studied.

the continuum mechanics modelling of the buckling of GaN NWs.

IV. BUCKLING OF GaN NWs

In this section, we will focus our attention on the axial buckling of GaN NWs. Fig. 6 shows the axial compression-strain relation for NWs with the electric field strength varying from $-0.2 \times 10^5 kV/cm$ to $0.2 \times 10^5 kV/cm$. In this section, the compressive axial stress and the compressive axial strain are taken as positive values. The images of the tested NW at different stages are shown in Fig. 7, which are associated with points A, B, and C on the stress-strain curve in Fig. 6. Initially, the axial stress monotonically increases with rising axial strain. When the strain reaches a certain critical value at point B the axial stress decreases rapidly with rising strain, indicating the onset of buckling in the NW. Thus, we define the strain at point B as the critical buckling strain and the associated stress is referred to as critical buckling stress. If the average axial strain is smaller than the critical value the NW is in stable equilibrium and retains a straight configuration; when the axial strain approaches the critical value (at point B), the NW is in a neutral equilibrium and the buckling is about to occur due to infinitesimal perturbation; at the axial strain larger than the critical value the NW becomes unstable.

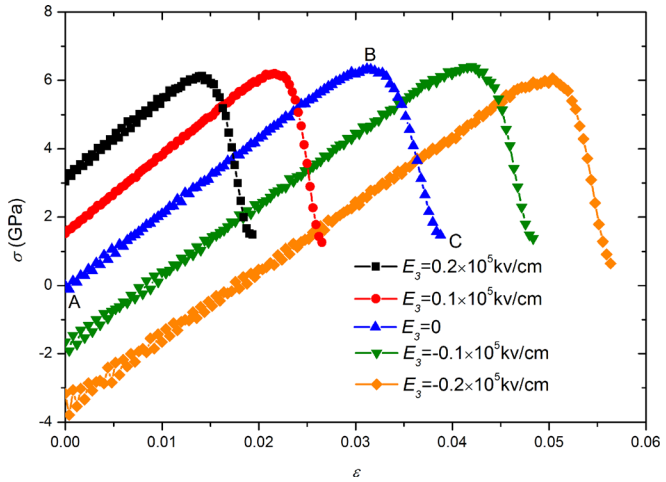

FIG. 6. Stress-strain curves for GaN NWs under a compression and different electric field strengths.

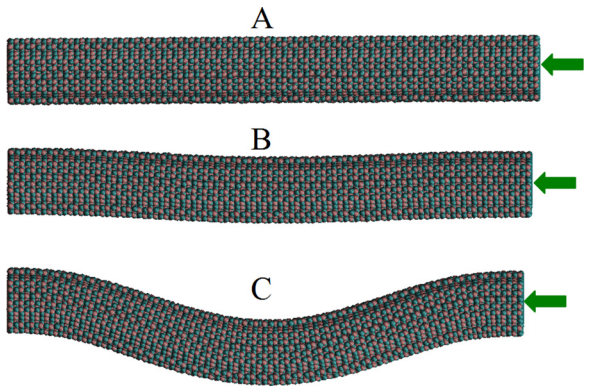

FIG. 7. Structures of GaN NWs under a compression from points A to C in Fig. 6.

The critical buckling stress and strain of the GaN NW under a compression are plotted in Fig. 8 as a function of the applied electric field. We can see from Fig. 8(a) that when the applied electric field increases from -0.2×10^5kV/cm to 0.2×10^5kV/cm the critical buckling stress is around 6.2 GPa with a variation less than $\pm 3\%$. In sharp contrast, as shown in Fig. 8(b), the critical buckling strain decreases almost linearly by 80% in the same process. To understand the observation in the MDS, we have resorted to the classical continuum mechanics theory. Based on the Timoshenko beam model, the governing equation for the buckling of the GaN NW reads[27]

$$EI\left(1-\frac{\sigma S}{kGS}\right)\frac{d^4w}{dx^4}+\sigma S\frac{d^2w}{dx^2}=0, \tag{3}$$

where w and x are the transverse displacement and the axial coordinate; G and k are the shear modulus and the shear correction coefficient; S and I are the area of cross-section and the second moment of the area. From the theory of piezoelectricity, the pre-buckling stress σ in Eq. (3) can be expressed as

$$\sigma = E\varepsilon + E_3 e_{33}. \tag{4}$$

For a fixed-fixed NW, the critical buckling stress σ_{cr} given by Eq. (3) is as follows:

$$\sigma_{cr} = \frac{4(\pi^2/L^2)EI}{S+4(\pi^2/L^2)(EI/kG)}, \tag{5}$$

which is found to be independent of the electric field E_3. Substituting Eq. (5) into Eq. (4) leads to the critical buckling strain ε_{cr} as

$$\varepsilon_{cr} = \frac{4(\pi^2/L^2)I}{S+4(\pi^2/L^2)(EI/kG)} - \frac{e_{33}}{E}E_3. \tag{6}$$

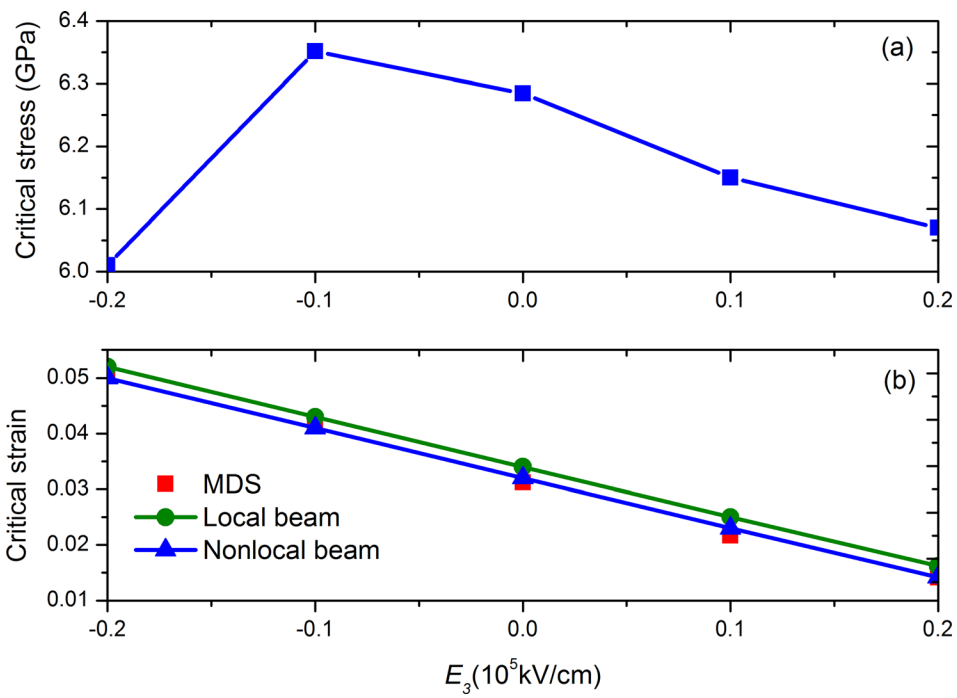

FIG. 8. (a) The critical buckling stress and (b) the critical buckling strain as a function of the electric field strength.

Equation (6) shows that the critical buckling strain of the GaN NW decreases linearly with rising electric field as a result of the equivalent pre-buckling strain $-e_{33}E_3/E$ due to the pre-buckling stress $e_{33}E_3$ and the fixed ends of the NW. This indeed reveals the physics of the linear E_3 dependency of ε_{cr} achieved in the MDS.

The critical buckling stress σ_{cr} given by Eq. (5) is 7 GPa and critical buckling strain ε_{cr} given by Eq. (6) as a function of E_3 is shown in Fig. 8(b). It is found that σ_{cr} given by the classical Timoshenko beam theory is 13% greater than 6.2 GPa obtained in the MDS. The relative difference between the two methods in predicting ε_{cr}, however, increases from 3.2% to 14.6% when E_3 rises form -0.2×10^5kV/cm to 0.2×10^5kV/cm. We believe that the nonlocal elasticity should be responsible for this discrepancy,[28,29] as the atomic theory of lattice dynamics and experimental observations on phonon dispersion showed that the stress at one reference point depends not only on the strain at that point but also on the strain at other points inside the domain. The buckling equation of the GaN NW derived by incorporating the nonlocal theory into the classical Timoshenko beam model is[30]

$$EI\frac{(e_0a)^2\sigma S}{kGS}\frac{d^6w}{dx^6}+EI\left[1-\frac{\sigma S}{kGS}-(e_0a)^2\frac{\sigma S}{EI}\right]\frac{d^4w}{dx^4}+\sigma S\frac{d^2w}{dx^2}=0, \tag{7}$$

where e_0a is the nonlocal coefficient characterizing the nonlocal effect on the response of the GaN NWs. The general solution to this singular equation takes the form[31]

$$w=C_1\cosh(\beta x)+C_2\sinh(\beta x)+C_3\cos(\eta x)+C_4\sin(\eta x), \tag{8}$$

where β and η are the functions of E, G, S, I, k, e_0a; and C_1 to C_4 are some real numbers. For fixed-fixed GaN NWs considered in this paper we have $w=0$ and $\phi=0$ at $x=0$ and L, here ϕ is the rotation angle and can be expressed in terms of w, i.e., $\phi=\phi(w)$. Substituting Eq. (8) into the boundary conditions yields $\mathbf{M}\cdot[C_1,C_2,C_3,C_4]^T=0$. Here, $\mathbf{M}$ is the coefficient matrix. The condition for nonzero solution of C_1 to C_4 is det$\mathbf{M}=0$, which gives the critical buckling stress of GaN NWs as well as the critical buckling strain. For more details on the method the reader may refer to Refs. 30 and 31.

The critical buckling stress of the GaN NW obtained from the nonlocal beam model is 6.4 GPa with the relative difference from the MDS result less than 3%. The value of e_0a associated with this good agreement is 1.1 nm. The critical buckling strain associated with $e_0a=1.1$nm is also plotted in Fig. 8(b) in comparison with the results of the MDS. A good agreement has been achieved throughout the length of the electric filed E_3 considered in the present study. The results show that the nonlocal effect is substantial for the GaN NWs and thus has to be considered in the analyses of their structural responses. In addition, it is noted that the value of the nonlocal coefficient $e_0a=1.1$nm is independent of the electric field applied although the nonlocal effect on ε_{cr} increases with rising E_3 (Fig. 8).

V. CONCLUSIONS

The effect of the electric field on the fracture and buckling of the GaN NWs has been investigated in the present study based on the MDS. The results show that the electric field has strong influence on the fracture strain and critical buckling strain. When the electric field changes from -0.4×10^5kV/cm to 0.4×10^5kV/cm the fracture strain increases by 47%. On the other hand, the increase of the electric field from -0.2×10^5kV/cm to 0.2×10^5kV/cm leads to the decrease of the critical buckling strain decrease by 72%. The effect of the electric field is found to be less pronounced for the fracture strength and almost negligible for the critical buckling stress. In addition, substantial nonlocal effect is achieved for the buckling responses of piezoelectric NWs studied here. In particular, $e_0a=1.1$nm is obtained for the GaN NWs. Accordingly, the nonlocal mechanics theory should be employed in studying the structural responses of the NWs. The obtained results suggest that applying an electric field can facilitate to maintain the structural integrity and stability of piezoelectric NWs via their piezoelectric effect.

ACKNOWLEDGMENTS

J.Z. acknowledges the support from the China Scholarship Council (CSC). S.A. acknowledges the support from the Royal Society through the award of Wolfson Research Merit Award.

[1]E. Comini, G. Faglia, G. Sberveglieri, Z. Pan, and Z. L. Wang, Appl. Phys. Lett. **81**, 1869 (2002).
[2]Y. Xi, C. G. Hu, X. Y. Han, Y. F. Xiong, P. X. Gao, and G. B. Liu, Solid State Commun. **141**, 506 (2007).
[3]X. D. Bai, P. X. Gao, Z. L. Wang, and E. G. Wang, Appl. Phys. Lett. **82**, 4806 (2003).
[4]X. D. Wang, J. Zhou, J. H. Song, J. Liu, N. S. Xu, and Z. L. Wang, Nano Lett. **6**, 2768 (2006).
[5]L. W. Ji, S. J. Young, T. H. Fang, and C. H. Liu, Appl. Phys. Lett. **90**, 033109 (2007)
[6]M. Riaz, O. Nur, M. Willander, and P. Klason, Appl. Phys. Lett. **92**, 103118 (2008).
[7]Z. G. Wang, X. T. Zu, L. Yang, F. Gao, and W. J. Weber, Physica E **40**, 561 (2008).
[8]Z. G. Wang, X. T. Zu, L. Yang, F. Gao, and W. J. Weber, Phys. Rev. B **76**, 045310 (2007).
[9]J. Y. Huang, H. Zheng, S. X. Mao, Q. M. Li, and G. T. Wang, Nano Lett. **11**, 1618 (2011).
[10]J. Zhang, R. J. Wang, and C. Y. Wang, Physica E **46**, 105 (2012).
[11]A. Bere and A. Serra, Philos. Mag. **86**, 2159 (2006).
[12]S. Nosé, J. Chem. Phys. **81**, 511 (1984).
[13]F. H. Stillinger and T. A. Weber, Phys. Rev. B **31**, 5262 (1985).
[14]M. Minary-Jolandan, R. A. Bernal, I. Kuljanishvili, V. Parpoil, and H. D. Espinosa, Nano Lett. **12**, 970 (2012).
[15]J. Zhang, C. Y. Wang, R. Chowdhury, and S. Adhikari, Scr. Mater. **68**, 627 (2013).
[16]S. J. Plimpton, J. Comput. Phys. **117**, 1 (1995).
[17]B. M. Wen, J. E. Sader, and J. J. Boland, Phys. Rev. Lett. **101**, 175502 (2008).
[18]R. Agrawal, B. Peng, and H. D. Espinosa, Nano Lett. **9**, 4177 (2009).
[19]K. W. Kang and W. Cai, Int. J. Plast. **26**, 1387 (2010).
[20]Z. S. Yuan, K. Nomura, and A. Nakano, Appl. Phys. Lett. **100**, 153116 (2012).
[21]K. Zheng, X. D. Han, L. H. Wang, Y. H. Yue, Y. F. Zhang, Y. Qin, X. N. Zhang, and Z. Zhang, Nano Lett. **9**, 2471 (2009).
[22]Z. X. Wu, Y. W. Zhang, M. H. Jhon, H. J. Gao, and D. J. Srolovitz, Nano Lett. **12**, 910 (2012).

[23]X. D. Han, K. Zheng, Y. F. Zhang, X. N. Zhang, Z. Zhang, and Z. L. Wang, Adv. Mater. **19**, 2112 (2007).
[24]J. Zhang, C. Y. Wang, R. Chowdhury, and S. Adhikari, Appl. Phys. Lett. **101**, 093109 (2012).
[25]V. V. Kochervinskii, Crystallogr. Rep. **48**, 649 (2003).
[26]S. X. Dai, M. Gharbi, P. Sharma, and H. S. Park, J. Appl. Phys. **110**, 104305 (2011).
[27]S. P. Timoshenko and J. M. Gere, *Theory of Elastic Stability* (McGraw-Hill, New York, 1961).
[28]A. C. Eringen, *Nonlocal Continuum Field Theories* (Springer-Verlag, New York, 2002).
[29]A. C. Eringen, J. Appl. Phys. **54**, 4703 (1983).
[30]J. Reddy and S. Pang, J. Appl. Phys. **103**, 023511 (2008).
[31]C. Y. Wang, J. Zhang, Y. Q. Fei, and T. Murmu, Int. J. Mech. Sci. **58**, 86 (2012).